



Contents lists available at ScienceDirect

Spectrochimica Acta Part A: Molecular and Biomolecular Spectroscopy

journal homepage: www.elsevier.com/locate/saa

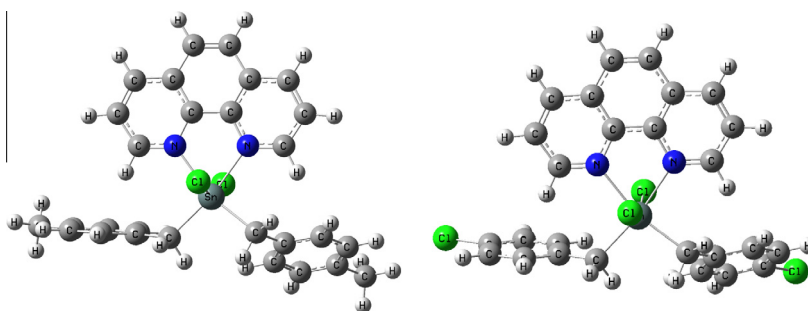
Synthesis, crystal structures HOMO–LUMO analysis and DFT calculation of new complexes of p-substituted dibenzyltin chlorides and 1,10-phenanthroline

S. Chandrasekar^{a,*}, V. Balachandran^b, Helen-Stoeckli Evans^c, A. Latha^a^a Department of Chemistry, Arignar Anna Government Arts College, Musiri, Tiruchirappalli 621 211, India^b Department of Physics, Arignar Anna Government Arts College, Musiri, Tiruchirappalli 621 211, India^c Institute of Physics, University of Neuchâtel, Rue Emile-Argand 11, CH-2009 Neuchâtel, Switzerland

HIGHLIGHTS

- New complexes of p-substituted dibenzyltin dichlorides are synthesized.
- Experimental FT-IR and FT-Raman spectra recorded for p-substituted dibenzyltin dichlorides.
- Quantum chemical analyses have been carried out for the first time.
- ¹H NMR, ¹³C NMR, ¹¹⁹Sn NMR spectra and X-ray crystallography were analyzed.
- Eventual charge transfer mechanism shown through HOMO and LUMO.

GRAPHICAL ABSTRACT



ARTICLE INFO

Article history:

Received 1 October 2014

Received in revised form 27 December 2014

Accepted 30 January 2015

Available online 9 February 2015

Keywords:

p-substituted dibenzyltin dichlorides
1,10-Phenanthroline
Crystal structures
Synthesis
DFT studies
HOMO–LUMO

ABSTRACT

In the present work, the complex formation of p-substituted dibenzyltin dichlorides with 1,10-phenanthroline. The reaction of (p-MeBz)₂SnCl₂ with 1,10-phenanthroline results (p-MeBz)₂SnCl₂-1,10-phenanthroline complex, (**2a**). Likewise (p-ClBz)₂SnCl₂ with 1,10-phenanthroline results (p-ClBz)₂SnCl₂-1,10-phenanthroline complex, (**2b**), in the similar reaction conditions. The IR, ¹H NMR, ¹³C NMR, ¹¹⁹Sn NMR spectral analyses indicate that the formation of hexacoordinated tin(IV) complexes in 1:1 ratio. The crystal structures of complexes **2a** and **2b** show that the tin atom is in regular octahedral geometry with the benzyl groups in the equidirectional positions. A comparison was made with the structural data of other R₂SnX₂-1,10-phenanthroline derivatives. Fourier transforms infrared and Raman spectral studies were performed for analyzing and assigning the vibrations and to identify the functional groups. Optimized geometrical parameters, harmonic vibrational frequencies, frontier molecular orbitals were obtained by DFT/B3LYP method combined with LanL2DZ basis set.

© 2015 Elsevier B.V. All rights reserved.

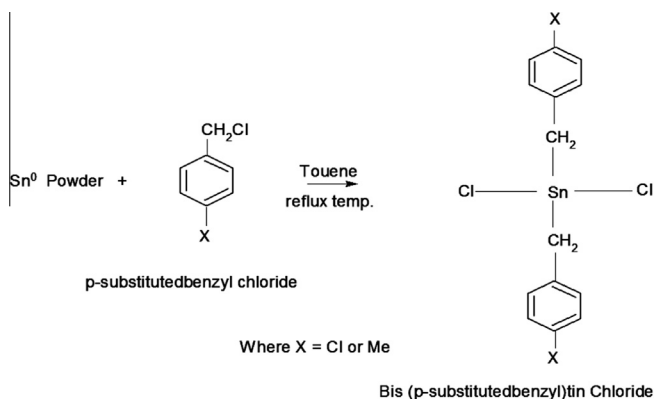
Introduction

Organotin(IV) derivatives have received much attention, both in academic and applied research, because of the ability of the tin to

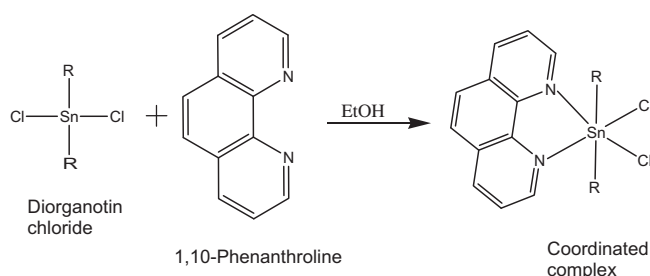
afford stable bonds with carbon as well as with hetero atoms; a wide range of compounds have been reported in organic synthesis and catalysis [1]. Furthermore, organotin(IV) complexes show a large spectrum of biological activities [2]. In recent years, several investigations to test their anti-tumor activities have been carried out and much attention has been focused on these properties and their implications in antioncogenesis [3]. It has been previously

* Corresponding author. Tel.: +91 4326260230, +914326262230; fax: +91 4326262630.

E-mail address: chand722002@yahoo.com (S. Chandrasekar).



Scheme 1. Synthesis of organotin(IV) compounds **1a** and **1b** [6].



2a : R = p-CH₃C₆H₄CH₂—

2b : R = p-ClC₆H₄CH₂—

Scheme 2. Synthesis of complexes, **2a** and **2b**.

reported that the 1:1 adducts formed between diorganotin dihalides and ligands with a N—C—C—N skeleton structure, like 2-aminomethyl pyridine and 1,10-phenanthroline, possess anti-tumor activity [4]. In our previous study, the crystal study of (dibenzyl dichloro)(1,10-phenanthroline)tin(IV) chloroform solvate complex was reported [5].

We report here on the synthesis of new organotin(IV) complexes made by the reaction of (p-MeBz)₂SnCl₂ or (p-ClBz)₂SnCl₂ with 1,10-phenanthroline in which tin is bound to the ligand as shown in Scheme 2. These two complexes, **2a** and **2b**, were characterized by IR, ¹H NMR, ¹³C NMR and ¹¹⁹Sn NMR spectra and X-ray crystallography. These studies revealed that the ligand is bound to the Sn(IV) atom through the nitrogen atoms.

The optimized geometry, vibrational wavenumbers and frontier molecular orbitals for the complexes **2a** and **2b** were calculated at DFT/B3LYP level of theory using LanL2DZ basis set. The results of the theoretical and spectroscopic studies are reported herein.

Experimental Techniques and computational methods

Experimental techniques

p-Methylbenzyl chloride, p-chlorobenzyl chloride, were commercially purchased from Lancaster Chemical Company, UK; 1,10-phenanthroline from qualigens; and is used without further purification; Tin powder from Loba Chemie; All solvents were dried according to a standard procedure.

Computational method

For the supportive evidence to the experimental observation, the density functional theory computations were performed with

the aid of GAUSSIAN 09W software package [6] with internally stored B3LYP/LanL2DZ basis set method. At first, the global minimum energy structures of the complexes were optimized by the aforesaid basis set method. Subsequently, the vibrational normal mode wavenumbers in association with the molecule were derived along with their IR intensities and Raman activities.

In our calculations, there were some deviations persist between the observed and calculated wavenumbers due to the neglect of anharmonic effect at the beginning of frequency calculations and basis set deficiencies. These deviations were overcome by a selective scaling procedure in the natural internal coordinate representation followed by Refs. [7,8]. Transformations of the force field and the subsequent normal coordinate analysis including the least squares refinement of the scaling factors, calculation of potential energy distribution (PED) and IR and Raman intensities were done on a PC with the MOLVIB program (Version V7.0-G77) written by Sundius [9,10]. The PED elements provide a measure of each internal coordinates contribution to the normal coordinate. In the present study, a selective scaling factor of 0.9961 is used for the wavenumbers less than 1700 cm⁻¹ and 0.9552 is used for greater than 1700 cm⁻¹.

Physical measurements

Melting points were obtained with Sigma instruments apparatus. The room temperature Fourier transform infrared spectra of the title compounds were measured in the region 4000–450 cm⁻¹, at a resolution ±1 cm⁻¹, using BRUKER IFS 66V vacuum Fourier transform spectrometer equipped with an MCT detector, a KBr beam splitter and globar source. The FT-Raman spectra were recorded on the same instrument with an FRA-106 Raman accessory in the region 3500–100 cm⁻¹. The 1064 nm Nd:YAG laser was used as excitation source, and the laser power was set to 200 mW. The observed FT-IR and FT-Raman spectra of the

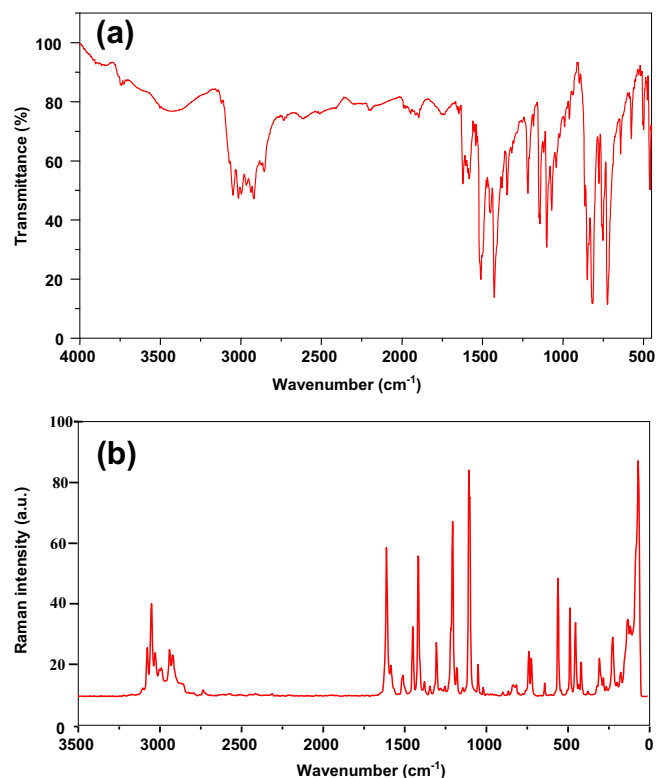


Fig. 1. Observed (a) FTIR (b) FT-Raman spectra of Bis(p-methylbenzyl)(1,10-phenanthroline)tin(IV) dichloro, complex **2a**.

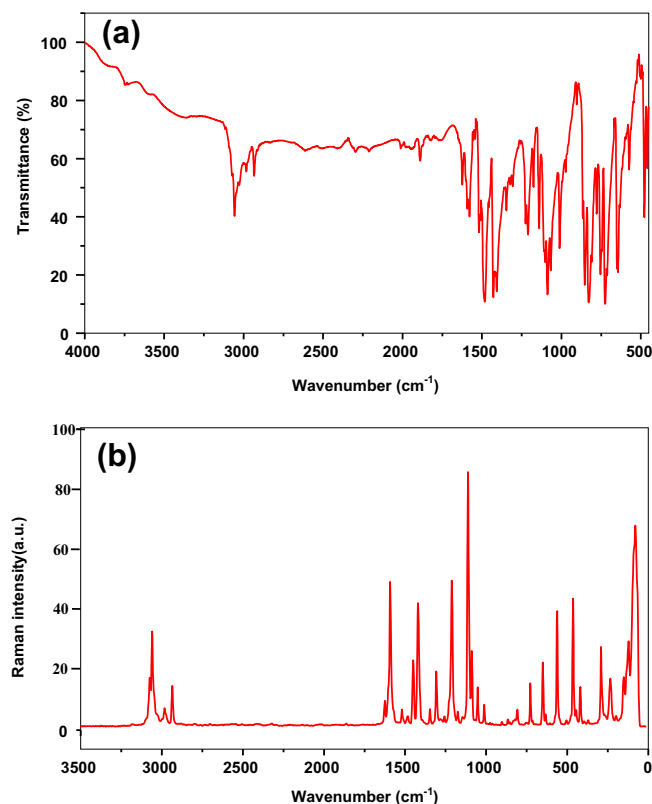


Fig. 2. Observed (a) FTIR (b) FT-Raman spectra of (p-chlorobenzyl)(dichloro)(1,10-phenanthroline)tin(IV), complex **2b**.

complexes **2a** and **2b** are shown in Figs. 1 and 2, respectively. ^1H , ^{13}C and ^{119}Sn NMR spectra were recorded at room temperature in CDCl_3 on a Bruker Avance 500 MHz. Me_4Si is used as external standard sample for ^1H and ^{13}C NMR spectra and for ^{119}Sn NMR, Me_4Sn is used as reference sample.

X-ray crystallography

Suitable crystals of **2a** and **2b** were obtained as pale-yellow plates and pale-yellow rods, respectively, by slow evaporation of solutions in chloroform. The intensity data were collected at 173 K on a Stoe Image Plate Diffraction System [11] using $\text{MoK}\alpha$

graphite monochromated radiation. Image plate distance 70 mm, ϕ oscillation scans 0 – 163° for **2a** and 0 – 186° for **2b**, with step $\Delta\phi = 1.3^\circ$, exposure time 6 min, 2θ range 3.27 – 52.1° . The structures were solved by direct methods using the program SHELXS-97 [12]. The refinement and all further calculations were carried out using SHELXL-97 [12]. The H-atoms were included in calculated positions and treated as riding atoms using SHELXL default parameters. The non-H atoms were refined anisotropically, using weighted full-matrix least-squares on F^2 . Empirical absorption corrections were applied using the multi-scan routine in PLATON [13]. Further crystallographic data and refinement details are given in Table 1. Selected bond distances and angles are given in Table 2.

Synthesis of bis(p-substituted benzyl)tin chlorides

Bis(p-methylbenzyl)tin dichloride, **1a**, and bis(p-chlorobenzyl)tin dichloride, **1b**, were prepared by the reactions of respective p-substituted benzyl halides with tin powder in toluene, isolated and purified as per the procedure reported in the literature (Scheme 1) [14].

Synthesis of bis(p-methylbenzyl)tin chloride, **1a**

4.0 g (0.034 mol) of tin powder, three drops (or 1–2% of the weight of tin) of water was added and kneaded together. The tin powder was suspended in 150 ml of toluene under efficient stirring and heated to the boiling point of the dispersing agent. To this suspension, 5.09 g (4.8 ml, d-1.062, 0.036 mol) of p-methylbenzyl chloride was added dropwise and refluxed for three hours. Yellow solid (6.5 g or 80%) and recrystallized from ethylacetate to give 5.5 g (75%) of white crystals with silky appearance. Extraction of the recovered tin powder (2 g or 0.016 mol) with water gave no inorganic salt. m.p. 230°C

^1H NMR δ ppm: 2.339, 6 H, CH_3 groups; 3.143, 2 H, $-\text{CH}_2$ groups; $^2J_{\text{Sn-H}} = 38.5$ Hz, 6.962, 2H; 6.977, 2H; 7.064, 2H; 7.080, 2H;

^{13}C NMR δ ppm: 21.04 (CH_3), 32.10 (CH_2), 128.17; 129.73 Aromatic Protons.

Synthesis of bis(p-chlorobenzyl)tin chloride, **1b**

The starting compound, **1b**, was prepared by similar procedures of the compound, **1a**. Tin powder 4.0 g (0.034 mol); Toluene 150 ml; p-chlorobenzyl chloride 6.12 g (4.8 ml, d-1.275, 0.038 mol), m.p: 218°C

Table 1
Crystallographic data and refinement details for compounds **2a** and **2b**.

Parameters	2a	2b
Chemical formula	$\text{C}_{28}\text{H}_{26}\text{Cl}_2\text{N}_2\text{Sn}$	$\text{C}_{26}\text{H}_{20}\text{Cl}_4\text{N}_2\text{Sn}$
M_r	580.10	620.93
Cell setting, space group	Monoclinic, $P2_1/n$	Monoclinic, $P2_1/c$
Temperature (K)	173(2)	173(2)
a, b, c (Å)	14.9580(14), 10.4051(7), 17.6819(16)	8.9639(8), 17.9723(11), 15.6964(15)
α, β, γ ($^\circ$)	90, 114.832(10), 90	90, 98.910(11), 90
V (Å ³)	2497.6(4)	2498.2(4)
Z	4	4
Radiation type	$\text{Mo K}\alpha$	$\text{Mo K}\alpha$
μ (mm ⁻¹)	1.26	1.47
Crystal size (mm)	$0.34 \times 0.30 \times 0.18$ mm	$0.38 \times 0.12 \times 0.08$ mm
Diffractometer	STOE IPDS diffractometer	STOE IPDS diffractometer
Absorption correction	Multi-scan	Multi-scan
$T_{\text{min}}, T_{\text{max}}$	0.647, 0.796	0.887, 0.893
R_{int}	0.031	0.030
$R[F^2 > 2\sigma(F^2)], wR(F^2), S$	0.024, 0.060, 0.93	0.023, 0.046, 0.85
No. of reflections	4884	4802
No. of parameters	300	298
H-atom treatment	H-atom parameters constrained	H-atom parameters constrained
$\Delta\rho_{\text{max}}, \Delta\rho_{\text{min}}$ (e Å ⁻³)	0.94, -0.71	0.37, -0.50

Table 2Selected experimental and calculated bond distances (Å) and bond angles (degrees) for compounds **2a** and **2b** based on B3LYP/LanL2DZ.

Parameters	Bond distances (Å)				Parameters	Bond angles (degrees)			
	Experimental		Calculated			Experimental		Calculated	
	2a	2b	2a	2b		2a	2b	2a	2b
Sn1–Cl1	2.53(7)	2.49(8)	2.41	2.40	Cl1–Sn1–Cl2	105.10(3)	105.63(3)	104.85	104.74
Sn1–Cl2	2.53(6)	2.53(8)	2.40	2.40	Cl1–Sn1–N1	92.73(5)	90.20(5)	91.90	88.09
Sn1–N1	2.35(18)	2.36(19)	2.31	2.30	Cl1–Sn1–N2	163.21(5)	160.72(5)	161.36	160.17
Sn1–N2	2.36(2)	2.37(2)	2.25	2.29	Cl1–Sn1–C13	88.34(6)	91.90(8)	88.07	90.63
Sn1–C13	2.16(3)	2.17(2)	2.16	2.16	Cl1–Sn1–C21(C20)	90.23(7)	93.41(8)	89.81	93.75
Sn1–C21(C20)	2.17(3)	2.16(2)	2.16	2.16	Cl2–Sn1–N1	161.99(5)	164.15(5)	160.23	162.06
					Cl2–Sn1–N2	91.67(5)	93.62(5)	91.44	92.21
					Cl2–Sn1–C13	91.46(6)	86.18(7)	91.18	85.10
					Cl2–Sn1–C21(C20)	87.04(6)	87.83(7)	82.04	82.43
					N1–Sn1–N2	70.49(7)	70.53(7)	69.53	70.04
					N1–Sn1–C13	91.63(8)	92.73(9)	90.37	92.17
					N1–Sn1–C21(C20)	90.38(8)	91.99(9)	89.48	90.53
					N2–Sn1–C13	92.08(8)	88.37(9)	91.87	87.21
					N2–Sn1–C21(C20)	89.86(9)	88.19(9)	88.52	88.01
					C13–Sn1–C21(C20)	177.59(9)	172.89(10)	175.36	171.43

^1H NMR δ ppm: 3.135, 2H, $-\text{CH}_2$ groups; $^2J_{\text{Sn-H}} = 47.5$ Hz, 7.036, 7.053, 7.218, 7.234.

^{13}C NMR δ ppm: 50.13 (CH_2 groups); 128.94, 129.70, Aromatic Protons.

Synthesis of complexes (**2a** and **2b**)

Synthesis of (*p*-methylbenzyl)(dichloro)(1,10-phenanthroline)tin(IV) complex, **2a**

To the solution of bis(*p*-methylbenzyl)tin chloride (0.1680 g, 0.00042 mol) in ethyl alcohol, 1,10-phenanthroline (0.083 g, 0.00042 mol) in ethyl alcohol was added drop wise using a pressure equalizing funnel. During the addition, the color of the reaction mixture slowly turned yellow and the mixture was allowed to stir for one hour. After the completion of the reaction, the solvent was removed completely in vacuum. A pale yellow solid was obtained. The obtained product was crystallized by vapor diffusion method as follows. The solid was dissolved in chloroform in a vial and was placed in a beaker containing petroleum ether. Crystals separated after two days. Yield = 0.2 g. 85%, m.p: 248 °C

^1H NMR δ ppm: s 1.799, 6H, CH_3 groups, s 3.271, 6H, 3 CH_2 groups, $^2J_{\text{Sn-H}} = 139$ Hz, s, 6.027 ppm, d 8.370; d 9.346 d 9.358. ^{13}C NMR δ ppm: 20.36 (CH_3), 51.15 (CH_2), 124.76, 126.76, 126.46, 126.95, 127.12, 127.28, 127.44, 127.68, 128.33, 133.10, 136.31, 138.54, 140.47, 148.70.

^{119}Sn NMR δ ppm: –338.508.

Point group: 2/m.

Synthesis of (*p*-chlorobenzyl)(dichloro)(1,10-phenanthroline)tin(IV) complex, **2b**

The complex, **2b**, was prepared by similar procedures of complex, **2a**. To the solution of is(*p*-chlorobenzyl)tin chloride (0.65 g, 0.0014 mol), 1,10-phenanthroline (0.29 g, 0.0014 mol) in ethyl alcohol was added drop wise using a pressure equalizing funnel. A yellow solid was obtained. Yield: 0.75 g, 80%, m.p = 245 °C

IR: KBr disc, cm^{-1} ν [(Sn–C)] 573.23, ν [(C–H)] 3057.70, ν [(Sn–N)] 475.38.

^1H NMR δ ppm: 3.216, 6H, 3 CH_2 groups, $^2J_{\text{Sn-H}} = 144$ Hz; m 6.128–6.050; m 6.204–6.245, q 7.823–7.797; doublet of doublet 8.492–8.473; doublet of doublet: 9.341–9.328.

^{13}C NMR δ ppm: 50.68, Sn- CH_2 ; 125.08, 126.39, 126.55, 126.71, 126.90, 128.94, 128.50, 128.70, 128.94, 129.47, 138.13, 139.24, 140.09, 148.59,

^{119}Sn NMR δ ppm: –343.823.

Point group: 2/m.

Results and discussion

Some new *p*-substituted organotin(IV) derivatives of 1,10-phenanthroline complexes were prepared by the reaction of the

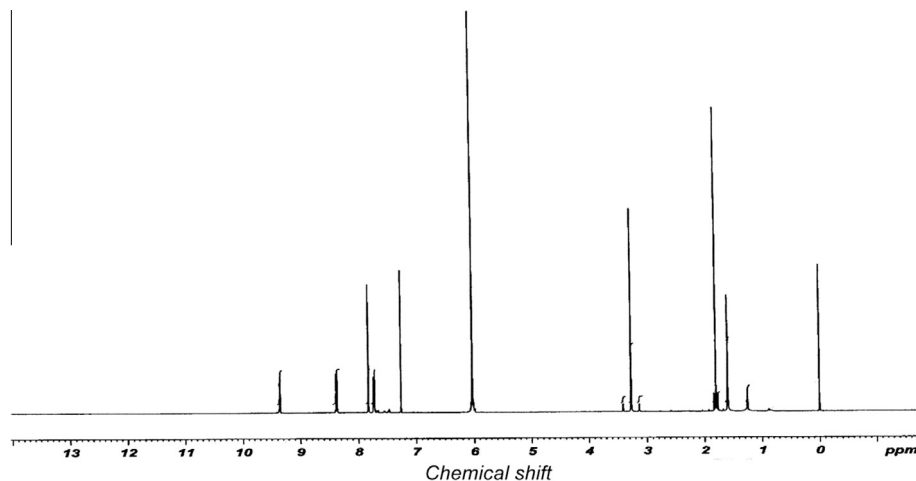


Fig. 3. ^1H NMR spectrum of the Bis(*p*-methylbenzyl)(dichloro)(1,10-phenanthroline)tin(IV), complex **2a**.

1,10-phenanthroline with selected p-substituted dibenzyltin(IV) chlorides in ethyl alcohol in appropriate mole ratio (Scheme 2).

Spectroscopic data

The complexes **2a** and **2b** were characterized by multinuclear (^1H , ^{13}C , ^{119}Sn) NMR, IR spectroscopy and X-ray analysis in combination with melting points.

The ^1H NMR spectra were recorded for the complexes **2a** and **2b** in CDCl_3 . The characteristic chemical shifts were identified by their intensity and multiplicity patterns. The total number of protons, calculated from the integration values, is in agreement with the expected molecular composition of the complexes. The proton chemical shifts assignment of the carbon attached to Sn exhibits a singlet at 3.271 ppm and at 3.216 ppm for complexes **2a** and **2b**. The

protons of the ligand and benzyl tin moieties for the complexes resonate as singlets, doublets and multiplets in the expected range 6.027–9.358 ppm [15]. The proton chemical shift assignment of the substituted dibenzyltin chloride moiety is a straight forward from the multiplicity pattern. The 2J [^{119}Sn – ^1H] coupling constant values for **2a** and **2b** complexes are 139 Hz and 144 Hz respectively. It supports the octahedral environment around Sn atom for the two complexes [16].

The ^{13}C NMR data explicitly resolved the resonances of all the distinct carbon atoms present in the complexes. The aromatic carbon resonances of the p-substituted benzyl moieties and the ligand of complexes, **2a** and **2b** are easily assigned on the basis of signal intensities. The aromatic carbon resonances were assigned by comparison of experimental chemical shift values [17]. The chemical shift values for p-substituted benzyl groups and the ligand of the

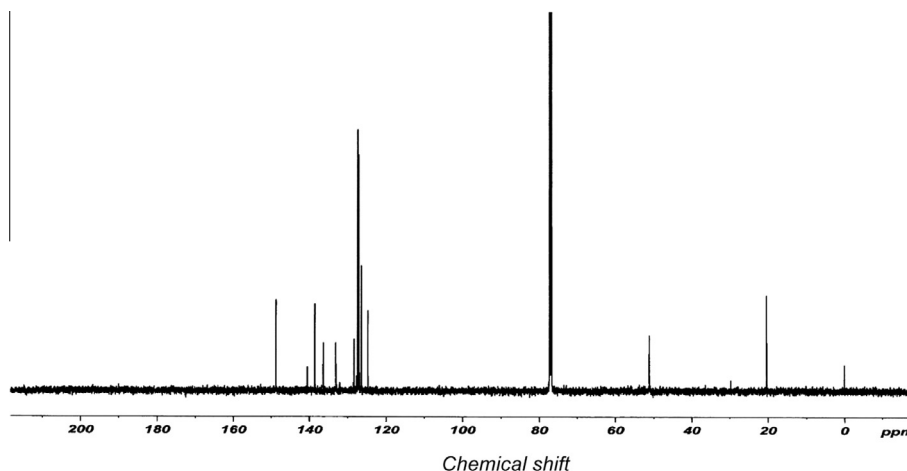


Fig. 4. ^{13}C NMR spectrum of the Bis(p-methylbenzyl)(dichloro)(1,10-phenanthroline)tin(IV), complex **2a**.

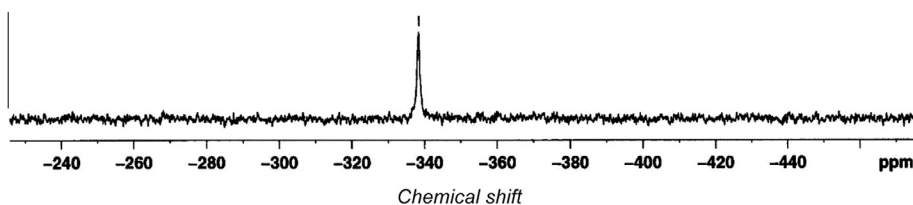


Fig. 5. ^{119}Sn NMR spectrum of the Bis(p-methylbenzyl)(dichloro)(1,10-phenanthroline)tin(IV), complex **2a**.

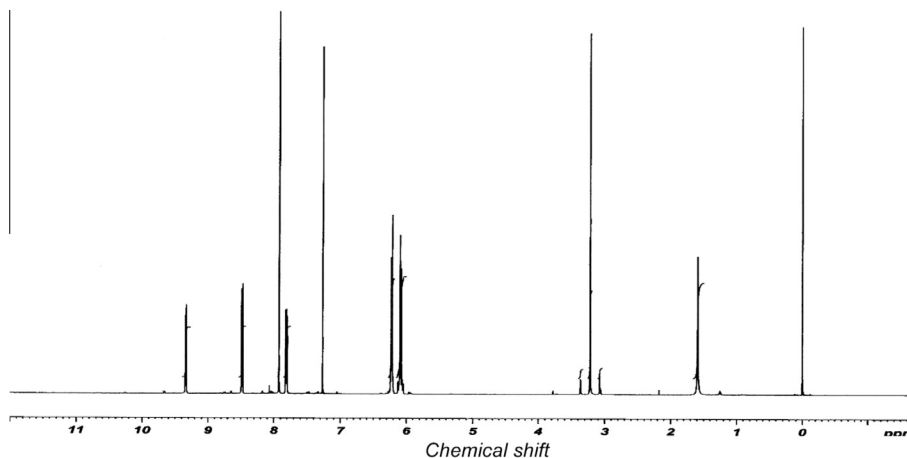


Fig. 6. ^1H NMR spectrum of the (p-chlorobenzyl)(dichloro)(1,10-phenanthroline)tin(IV), complex **2b**.

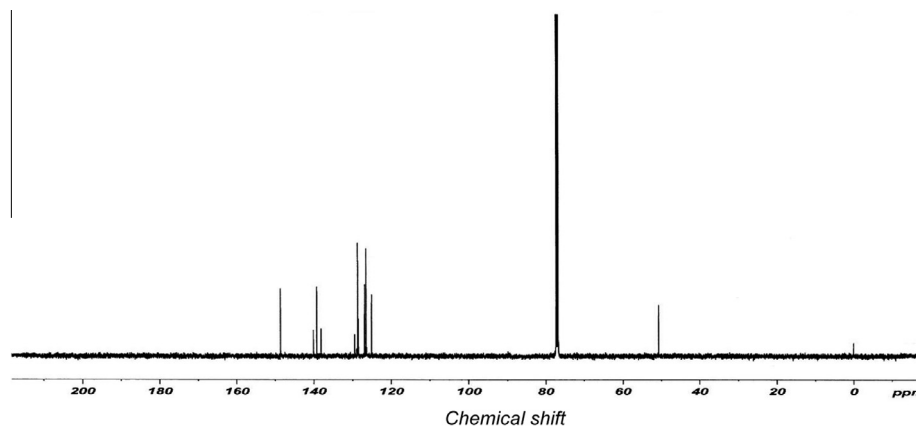


Fig. 7. ^{13}C NMR spectrum of the (p-chlorobenzyl)(dichloro)(1,10-phenanthroline)tin(IV), complex **2b**.

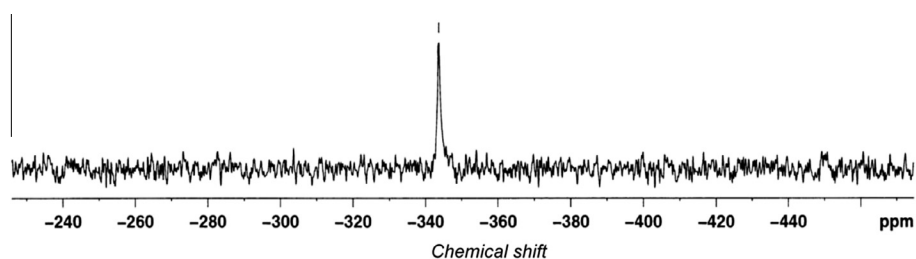


Fig. 8. ^{119}Sn NMR spectrum of the (p-chlorobenzyl)(dichloro)(1,10-phenanthroline)tin(IV), complex **2b**.

complexes, **2a** and **2b**, give signals in the expected range of 124.76–148.70 ppm [18]. From the ^{13}C NMR, the formation of the complex is confirmed by the change in the chemical shift observed for the methylene group at 51.15 ppm and at 50.68 ppm observed for the same carbon of bis(p-substituted benzyl)tin chloride for the complexes, **2a** and **2b**. The fact that only one signal is obtained for the above carbon indicate the equivalence of the two methylene groups in the two complexes.

The experimental and theoretical ^{119}Sn NMR data (in CDCl_3) show a single resonance at -338.508 ppm and -335.316 ppm for bis(p-methylbenzyl)(dichloro)(1,10-phenanthroline)tin(IV) **2a**, and at -343.823 ppm and -340.274 ppm for (p-chlorobenzyl)(dichloro)(1,10-phenanthroline)tin(IV) **2b**, complexes. These values are in conformity to hexa coordination around the Sn atom as reported earlier [19]. The chemical shift values observed for these complexes are comparable with corresponding values for similar complexes [20]. This up field signal is attributed to high electron density on tin because of complexation in these complexes [21]. This feature has been confirmed by single crystal XRD studies when two complexes were crystallized in CHCl_3 by solvent diffusion method. The observed ^1H , ^{13}C , and ^{119}Sn NMR spectra of the complexes **2a** and **2b** and its assignments are shown in Figs. 3–8.

Crystallographic study

Figs. 9 and 10 show the ORTEP and Gaussview representation of the molecular structures for the complexes, **2a** and **2b**. The crystallographic data, refinement details, the selected bond lengths and angles along with the theoretical values for the crystals of these complexes are listed in Table 1 and Table 2. There are four independent molecules in the asymmetric unit in both **2a** and **2b** and are discussed here. Tin atom is surrounded by two carbon atoms, two chlorines and two nitrogens in octahedral environment. Bidentate nitrogen donor ligand and two chlorines are in equatorial positions and two carbons of benzyl groups are in axial positions in these two complexes.

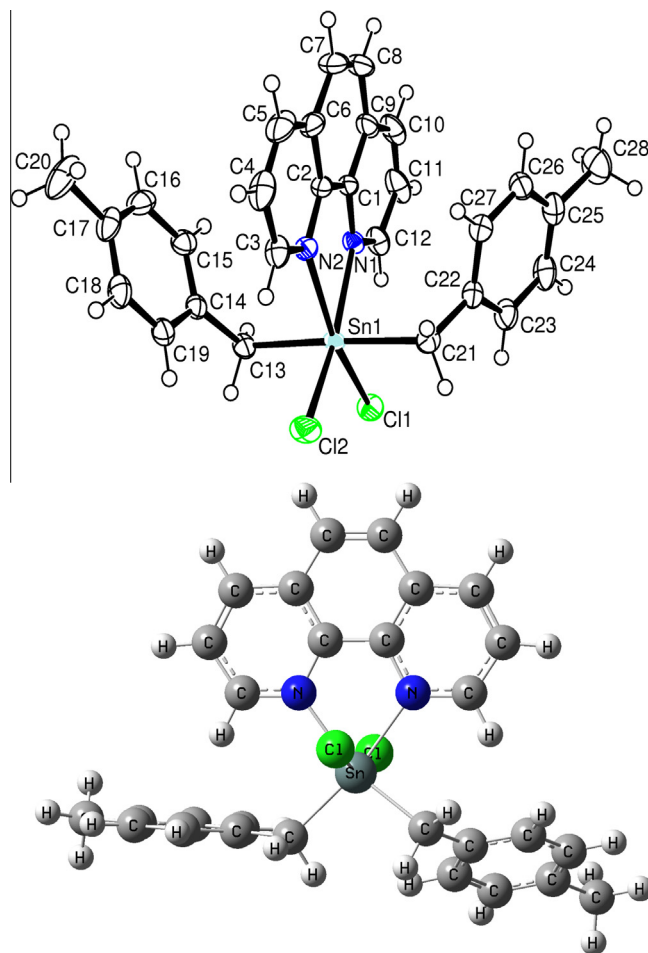


Fig. 9. The crystal structure of Bis(p-methylbenzyl)(dichloro)(1,10-phenanthroline)tin(IV), complex **2a**.

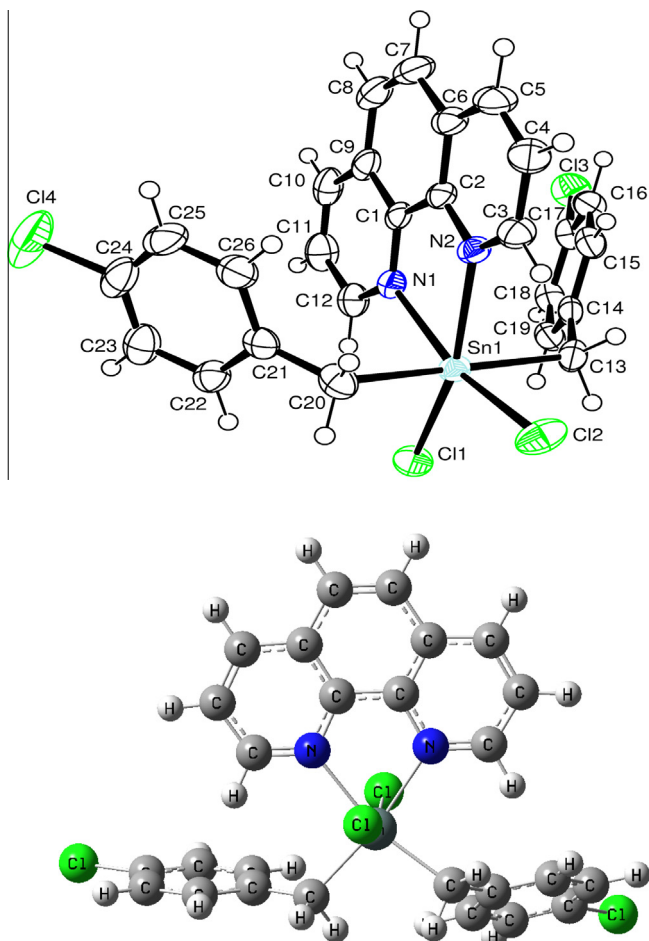


Fig. 10. The crystal structure of (p-chlorobenzyl)(dichloro)(1,10-phenanthroline)tin(IV), complex **2b**.

All the Sn bond lengths are close or very close to the mean Sn–Cl, Sn–C, Sn–N distances reported in a recent review of diorganodihalotin complexes [5,22,23]. The Sn–Cl distances are 2.5289(7) Å and 2.5325(6) Å; 2.4941(8) Å and 2.5278(8) Å; in **2a** & **2b** respectively lies in the range (2.32–2.58 Å) of Sn–Cl distances found in chloroorganotin(IV) complexes in general [24–26]. The Sn–N bond lengths are 2.3497(21) Å and 2.362(2) in **2a** and 2.3575(26) and 2.370 Å (2) in **2b** are shorter than the complexes [27]. They are longer than the sum of the covalent radii of tin and nitrogen (2.15 Å) and significantly shorter than the sum of their van der Waals radii (3.75 Å) and thus indicating a substantial bonding interaction [28]. The Sn–C distances 2.161(3) Å and 2.169(3) Å in **2a**; 2.165(2) Å and 2.161(2) Å in **2b** are quite close to those found in similar type of complexes [29–33].

A significant distortion in octahedral geometry arises from the presence of the bridged ligand. Thus, owing to the coordination angles between each respective *trans* groups are not equal to 180°, the benzyl groups are not precisely perpendicular to the plane [Cl(1)–Sn–Cl(2), 105.10(3) and N(1)–Sn–N(2), 70.49(7)] in the complex **2a** and [Cl(1)–Sn–Cl(2), 105.63(3) and N(1)–Sn–N(2), 70.53(7)] in the complex **2b**. The deviation from the regular octahedral geometry (C(13)–Sn–C(20) 172.89(10)) in **2b**, may result from the electronegative Cl atoms attached to *p*-positions of both benzyl groups which are bonded to tin atom in axial positions.

Molecular electrostatic potential

Molecular electrostatic potential (MEP) is a plot of electrostatic potential mapped on to the constant electron density surface. MEP

displays molecular size, shape and electrostatic potential value. Electrostatic potential correlates with dipole moment, electronegativity, partial charges and site of chemical reactivity of the molecule. It provides a visual method to understand the relative polarity of a molecule. The negative electrostatic potential corresponds to an attraction of the proton by the concentrated electron density in the molecule. The positive electrostatic potential corresponds to repulsion of the proton by the atomic nuclei in regions where low electron density exist and the nuclear charge is incompletely shielded. By definition, electron density isosurface is a surface on which molecule's electron density has a particular value and that encloses a specified fraction of the molecule's electron probability density [34–36]. The electrostatic potential values are represented by different colors. The positive, negative and neutral electrostatic potential regions of molecules are shown in terms of color grading. Potential increases in the order red < orange < yellow < green < blue. Generally the red color indicates the maximum negative region and the blue color represents the maximum positive region. To predict reactive sites for electrophilic and nucleophilic attack for the investigated molecule, MEP surface is plotted over optimized geometry of both **2a** and **2b** at B3LYP/LanL2DZ basis set [37,38]. Figs. 5 and 6 shows electrostatic potential contour map of **2a** and **2b** along with the fitting point charges to the electrostatic potential. In the present study, the value of point charges to the electrostatic potential are predicted with the help of B3LYP level of the theory incorporating 6–31G(d, p) basis set. As easily can be seen in

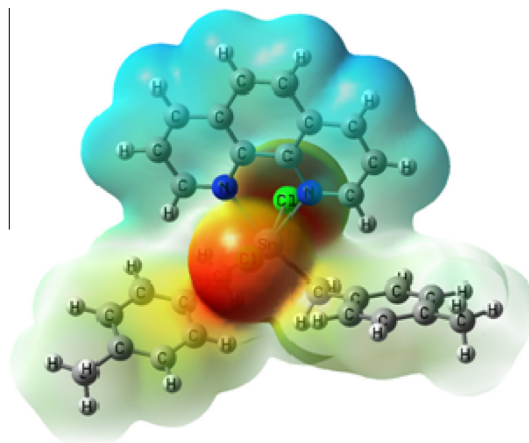


Fig. 11. Electrostatic potential surface map of Bis(p-methylbenzyl)(dichloro)(1,10-phenanthroline)tin(IV), complex **2a**.

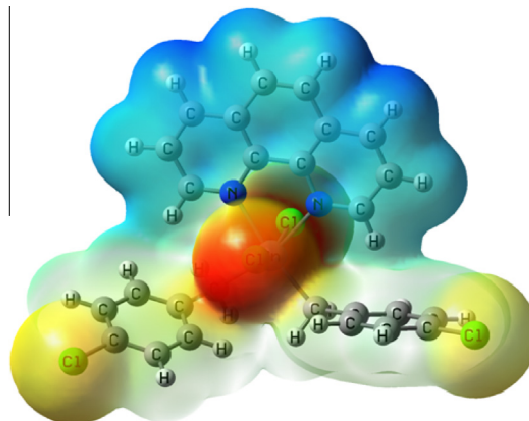


Fig. 12. Electrostatic potential surface map of (p-chlorobenzyl)(dichloro)(1,10-phenanthroline)tin(IV), complex **2b**.

Figs. 11 and 12, investigated molecule has several possible sites for electrophilic (the electrophilic sites are most electro negative and are represented as red color) and nucleophilic attack (the nucleophilic sites are most positive and are represented as blue color).

HOMO and LUMO analysis

The energies of the highest occupied molecular orbital (HOMO) and the lowest unoccupied molecular orbital (LUMO) are computed at B3LYP/LanL2DZ level. HOMO and LUMO orbitals for the complexes **2a** and **2b** are shown in Figs. 13 and 14, respectively. Generally the energy values of LUMO, HOMO and their energy gap reflect the chemical activity of the molecule. HOMO as an electron donor represents the ability to donate an electron, while LUMO as an electron acceptor represent the ability to receive an electron [39,40]. The energies of the HOMO [−0.21780 eV, 0.12788 eV] and LUMO [−5.12 eV, 0.11751 eV] and the energy gaps are found to be 0.33888 eV and 0.35783 eV. The HOMO–LUMO energy gap reveals the intramolecular charge transfer (ICT) interaction occurs within the molecule.

Vibrational spectral analysis

C–H vibrations

The aromatic ring stretching vibrations are normally found between 3100 and 2900 cm^{-1} [41]. The C–H stretching vibrations

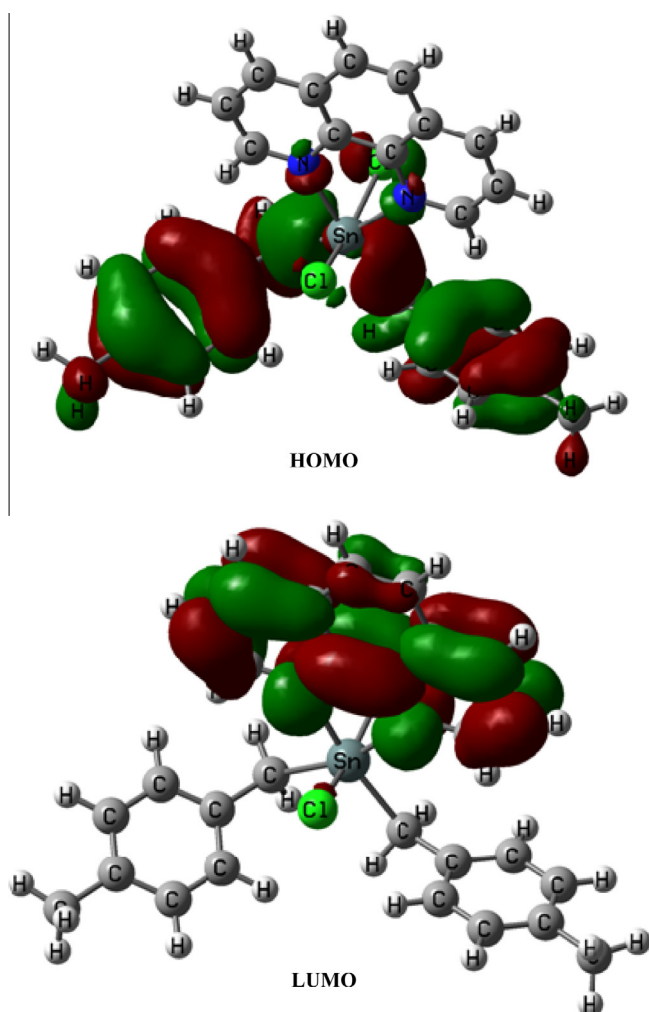


Fig. 13. Frontier molecular orbitals of Bis(p-methylbenzyl)(dichloro)(1,10-phenanthroline)tin(IV), complex **2a**.

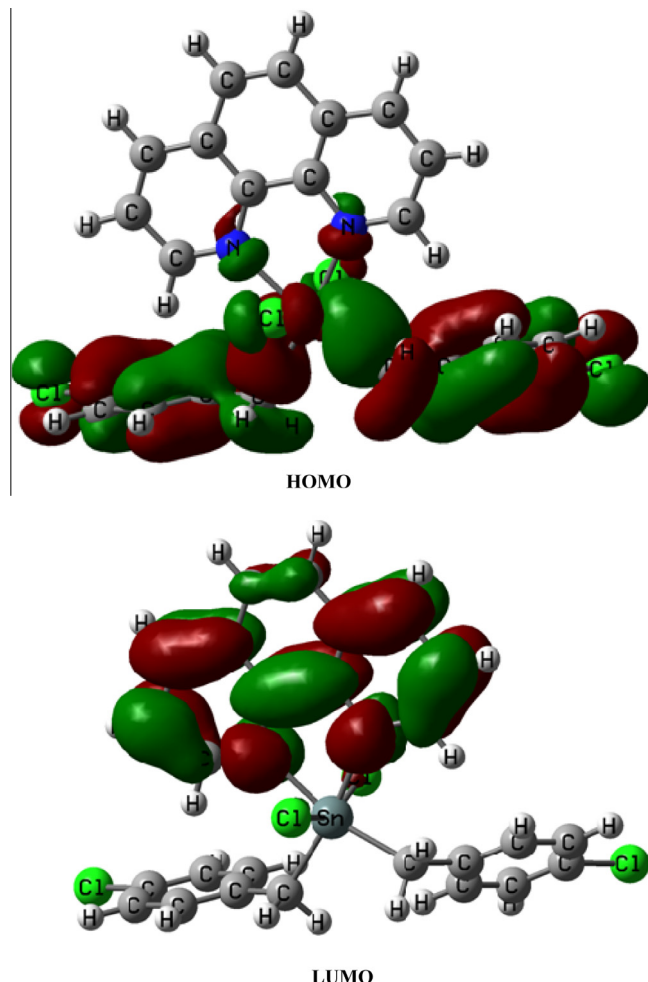


Fig. 14. Frontier molecular orbitals of (p-chlorobenzyl)(dichloro)(1,10-phenanthroline)tin(IV), complex **2b**.

of **2a** are observed in 3148, 3142, 3077, 3051, 2991, 2940 and 2921 cm^{-1} in FT-Raman spectrum and 3047, 3040, 3015, 3009, 2986, 2959, and 2912 cm^{-1} in FT-IR spectrum. The bands 3193, 3074, 3054, 3019 cm^{-1} in Raman spectrum and 3093, 3059, 3010, 2994 cm^{-1} in FT-IR spectrum are assigned to C–H stretching vibrations for the complex **2b**. The C–H in-plane and out-of-plane bending vibrations modes are found to be well within the characteristic region.

CH₃ vibrations

For the assignments of CH₃ group frequencies, basically nine fundamentals can be associated to each CH₃ [32], group namely, CH₃ss: symmetric stretch; CH₃ips: in-plane stretch (i.e. in-plane hydrogen stretching modes); CH₃ipb: in-plane-bending (i.e., hydrogen deformation modes); CH₃sb: symmetric bending; CH₃-ipr: in-plane rocking; CH₃opr: out-of-plane rocking and tCH₃: twisting hydrogen bending modes. In addition to that, CH₃ops: out-of-plane stretching and CH₃opb: out-of-plane bending modes of the CH₃ group would be expected to be depolarized for A' symmetry species. Methyl groups are generally referred as electron-donating substituent in the aromatic ring systems. The methyl hydrogen atoms in complex **2a** are subjected simultaneously to hyper conjugation and back donation, which causes the decrease in stretching wavenumbers and infrared intensities, as reported in literature [42,43] for similar molecular system. For the CH₃ group compounds the asymmetric stretching mode appears in

Table 3
Selected experimental and calculated wavenumbers (cm^{-1}) and assignments, IR intensities (I_{IR}) and Raman activities (A_{Raman}) for compounds 2a and 2b based on B3LYP/LanL2DZ.

2a						2b					
Wavenumbers					Assignments /(PED%)	Wavenumbers					Assignments /(PED%)
FT-IR	FT-Raman	Calculated [#] (Scaled)	I_{IR}	A_{Raman}		FT-IR	FT-Raman	Calculated [#] (Scaled)	I_{IR}	A_{Raman}	
3148vw		3146	80.95	36.66	vCH(99)	3093w	3093w	3095	52.13	45.28	vCH(99)
	3142vw	3140	74.31	33.01	vCH(99)	3088ms		3090	70.15	34.98	vCH(99)
	3112vw	3110	0.68	74.55	v _{ass} CH ₃ (95)		3074ms	3076	3.45	75.25	vCH(99)
3093w		3096	0.54	87.62	v _{ass} CH ₃ (94)	3059vw		3060	12.05	59.68	vCH(99)
	3077ms	3074	26.98	80.92	vCH(98)		3054w	3052	16.25	50.07	vCH(98)
	3051vs	3050	6.60	73.76	vCH(98)		3019w	3022	4.08	55.42	vCH(98)
3047w		3046	59.62	46.49	vCH(97)	3010vw		3012	8.10	28.35	vCH(98)
3040w		3041	92.19	46.83	vCH(97)	2994w		2993	6.62	48.21	vCH(97)
	3028ms	3026	1.11	60.95	vCH(97)		2982vw	2981	41.97	29.14	vCH(98)
	3021vw	3020	1.19	43.46	v _{ass} CH ₃ (92)	2936vw		2936	31.25	39.36	v _{ass} CH ₂ (96)
3015w		3016	1.46	44.01	v _{ass} CH ₃ (91)		2928vw	2631	40.19	40.27	v _{ass} CH ₂ (96)
3009w		3006	2.65	50.02	vCH(98)	2858vw		2856	1.58	31.05	v _{ss} CH ₂ (94)
	2991vw	2990	9.82	59.52	vCH(98)		2844vw	2840	1.25	29.80	v _{ss} CH ₂ (94)
2986w		2989	2.04	60.81	vCH(98)						
2959w		2955	0.91	55.59	vCH(98)						
	2940ms	2941	39.07	12.59	vCH(98)						
	2921ms	2922	0.87	16.25	vCH(98)						
2912w		2911	0.82	28.32	v _{ass} CH ₂ (96)						
2906w		2906	0.08	29.97	v _{ass} CH ₂ (94)						
2855w		2854	1.21	72.22	v _{ss} CH ₃ (89)						
	2822vw	2821	2.79	24.38	v _{ss} CH ₃ (89)						
	2790vw	2793	2.94	71.13	v _{ss} CH ₂ (86)	1679w		1680	1.14	58.31	vCC(65), δ CH(21)
	2735vw	2734	4.44	65.46	v _{ss} CH ₂ (86)	1653w		1652	7.26	60.32	vCC(66), δ CH(21)
1666vw		1665	5.95	14.18	vCC(68), δ CH(21)	1639ms		1640	8.62	19.62	vCC(68), δ CH(20)
1621w		1620	7.08	14.78	vCC(68), δ CH(20)	1623ms	1624s	1625	4.98	5.48	vCC(65), δ CH(18)
1613vw	1612vs	1613	27.57	11.51	vCC(65), δ CH(18)	1592ms	1591w	1592	0.58	3.96	vCC(66), δ CH(20)
1584w	1583vw	1582	8.66	6.39	CH ₂ sciss.(86)	1578ms		1579	5.83	17.86	CH ₂ sciss.(86)
1573w		1575	4.94	19.64	CH ₂ sciss.(86)	1555ms		1554	1.23	12.62	CH ₂ sciss.(86)
1541vw		1540	0.59	25.11	δ_{opb} CH ₃ (87)	1542ms		1540	0.20	21.08	vCC(64), δ CH(20)
	1532vw	1533	5.80	3.96	δ_{opb} CH ₃ (86)				0.07	2.95	
	1514w	1512	2.74	31.79	δ_{ipb} CH ₃ (84)	1518s	1518w	1519	0.64	22.37	vCC(64), δ CH(21)
1509vs		1511	3.21	0.06	δ_{ipb} CH ₃ (84)	1508s		1510	2.68	1.19	vCC(66), δ CH(19)
1466vw		1465	8.32	17.86	vCN(67), vCC(20)	1482vs	1483ms	1483	5.57	1.38	vCC(58), δ CH(20)
1451ms	1451s	1450	13.75	18.04	δ_{sb} CH ₃ (80)	1450s	1449s	1451	13.69	2.92	vCN(58), δ CH(20)
1427vs		1428	1.23	83.48	δ_{sb} CH ₃ (80)	1428s		1430	2.75	1.08	vCN(66), δ CH(18)
	1417vs	1418	5.52	0.83	vCN(66), δ CH(22)	1413w	1419ms	1415	3.21	0.97	vCN(66), δ CH(18)
1378w	1379w	1380	4.04	0.72	vCN(64), δ CH(18)	1373w		1374	8.25	0.55	vCN(65), δ CH(20)
1347ms	1346w	1348	8.10	12.90	vCN(63), δ CH(18)	1346w	1346ms	1345	22.79	1.32	vCC(66), δ CH(20)
1319w		1318	6.56	35.13	CH ₂ rock.(69)	1321w		1320	1.32	0.99	CH ₂ rock.(69)
1306w	1306ms	1304	1.57	5.70	CH ₂ rock.(69)	1306w	1307w	1308	9.93	4.25	CH ₂ rock.(69)
1253w	1254vw	1253	1.21	1.78	CH ₂ wagg.(59)	1266w	1267vw	1269	2.48	1.19	CH ₂ wagg.(59)
1218s		1218	1.32	6.16	CH ₂ wagg.(59)	1225w	1221s	1224	1.69	0.83	CH ₂ wagg.(59)
1144s	1144w	1145	0.70	4.16	δ_{opr} CH ₃ (61)	753w	758ms	726	4.02	0.75	vCCI(73), δ CH(16)
1140vw		1138	3.36	4.65	δ_{opr} CH ₃ (60)	724ms	724w	651	7.71	3.33	vCCI(73), δ CH(16)
1119w		1121	1.62	7.05	δ_{ipr} CH ₃ (72)	649ms	650ms	401	0.86	4.25	vCC(66), δ CH(18)
1107s		1106	0.58	1.38	δ_{ipr} CH ₃ (99)	399ms		364	5.24	0.16	vSnCl(58)
	378vw	379	0.99	0.09	vSnCl(58)	366ms		290	2.11	0.30	vSnCl(58)
	307w	308	0.03	0.19	vSnCl(58)		291ms	265	0.47	0.24	CH ₂ twist.(56)
	283w	282	0.08	0.12	CH ₂ twist.(56)		266ms		0.71	0.15	CH ₂ twist.(56)
	265w	262	0.14	0.30	CH ₂ twist.(56)						
	133vw	133	0.05	0.97	τ CH ₃ (55)						
	118w	116	0.01	0.17	τ CH ₃ (5)						

v: stretching; δ : deformation; τ : twisting; ass: asymmetric stretching; ss: symmetric stretching; opb: out-of-plane bending; ipb: in-plane bending; sb: symmetric bending; rock.: rocking; sciss.: scissoring; wagg.: wagging; twist: twisting.

[#] Scale factor of 0.9961 is used for the wavenumbers less than 1700 cm^{-1} and 0.9552 is used for greater than 1700 cm^{-1} .

the range 2825–2870 cm^{-1} , lower in magnitude compared with the value in CH_3 compounds (2860–2935 cm^{-1}) whereas the asymmetric stretching modes for the complex **2a** lie in the same region 2924 and 2985 cm^{-1} . The asymmetric and symmetric stretching vibrations of CH_3 group have been identified in 3112, 3093, 3021, 3015 cm^{-1} . Methyl groups are generally referred as electron-donating substituent in the aromatic ring systems. The observed asymmetric and symmetric CH_3 deformations vibrations for the complex **2a** are listed in the Table 3.

CH₂ vibrations

For the assignments of CH_2 group frequencies, basically six fundamentals can be associated with each CH_2 group namely, CH_2 symmetric stretch; CH_2 asymmetric stretch; CH_2 scissoring and CH_2 rocking, which belong to in-plane vibrations and two out-of-plane vibrations, viz., CH_2 wagging and CH_2 twisting modes, which are expected to be depolarized. The asymmetric CH_2 stretching vibrations are generally observed above 3000 cm^{-1} , while the symmetric stretch will appear between 3000 and 2900 cm^{-1} [44,45]. In the title complexes, the band at 2912, 2906 and 2936, 2928 cm^{-1} in FT-IR spectra is assigned to CH_2 asymmetric stretching modes for the complexes **2a** and **2b**, respectively. The medium strong band at 2790, 2735 cm^{-1} and 2858, 2844 cm^{-1} in FT-Raman are attributed to CH_2 symmetric stretching. Theoretically value at 2911, 2906, 2936, 2631 and 2793, 2735, 2856 and 2840 cm^{-1} by B3LYP/LanL2DZ method exactly correlate with the experimental observations.

Aromatic CH_2 compounds have a band of weak-to-medium intensity of 1500–200 cm^{-1} belong to CH_2 bending vibrations [42]. The CH_2 group of the complex is capable of different bending vibrations such as scissoring, wagging, rocking and twisting. These vibrations give rise to variable intensity bands at lower wavenumber region. In the present study, the prominent bands at 1584, 1573, 1578, 1555 cm^{-1} in FT-IR spectrum 1583 cm^{-1} in FT-Raman spectrum are assigned to CH_2 scissoring mode. In aromatic complexes, the wagging modes are expected in the region 1200 – 1000 cm^{-1} with a moderate to strong intensity. For the complexes **2a** and **2b**, the weak bands at 1253, 1218 cm^{-1} in IR and 1254 cm^{-1} in Raman and 1266, 1225 cm^{-1} IR and 1267, 1221 cm^{-1} in Raman are assigned to CH_2

C–Cl vibrations

The C–Cl stretching mode appears as mixed mode. In the lower region, C–Cl stretching vibrations appear in the region 760–505 cm^{-1} and C–Cl deformation vibrations appear in the region 420–250 cm^{-1} . For simple chlorine compounds, C–Cl absorption is in the region 750–700 cm^{-1} [42]. From the above literature the band observed at 753, 724 cm^{-1} in FT-IR spectrum are assigned to C–Cl stretching vibrations. The shift of lower frequency of **2b** is due to much greater electronegativity of Cl as compared to carbon atoms. Thus Cl atom acquires small positive charge and the carbon atom acquires small negative charge. The inductive effect of chlorine attracts electrons from C–Cl bond, which increases the force constants and leads to an increase in the absorption frequency.

Sn–C and Sn–Cl vibrations

Infrared-spectroscopy has provided valuable information on the molecular geometry of organotin compounds. Particularly important is the criterion established for determining the configuration of SnC_3 and SnC_2 moieties in chlorotrimethyltin and dichlorodimethyltin derivatives. Characteristic infrared absorptions of some tin-ligand stretching vibrations are $\nu(\text{Sn–C})$, 600–470 cm^{-1} and $\nu(\text{Sn–Cl})$, 390–310 cm^{-1} [46]. Hence, in the present study, the Sn–C stretching vibrations are observed at 562, 488 cm^{-1} and 562, 464 cm^{-1} in FT-Raman spectra for **2a** and **2b**

complexes, respectively. Similarly the Sn–Cl stretching vibrations for the complexes **2a** and **2b** are observed at 378, 307 cm^{-1} and 399, 366 cm^{-1} in FT-Raman spectra, respectively.

CC vibrations

The ring C=C and C–C stretching vibrations, known as semicircle stretching usually occur in the region 1625–1400 cm^{-1} . Hence in the present study, the FT-IR bands identified at 1666, 1621, 1613 cm^{-1} and the FT-Raman band at 1612 cm^{-1} are assigned to C–C stretching vibrations of the complex **2a**. The bands ascribed at 1679, 1653, 1639, 1623, 1592, 1542, 1518, 1508, 1482, 1346 cm^{-1} in FT-IR spectrum and 1624, 1591, 1518, 1483, 1346 cm^{-1} in FT-Raman have been designated to C–C stretching modes for the complex **2b**. The theoretically calculated C–C stretching modes for the complexes **2a** and **2b** are found at 1665, 1620, 1613, 1465 cm^{-1} and 1680, 1652, 1640, 1625, 1592, 1540, 1519, 1483, 1345 cm^{-1} , respectively.

CN vibrations

The identification of C–N vibration is a difficult task, since the mixing of vibrations is possible in their region. In the present work, the bands observed at 1466, 1378, 1347 cm^{-1} in FT-IR spectrum and 1417, 1379, 1346 cm^{-1} in FT-Raman spectrum are assigned to C–N stretching vibrations for the complex **2a**. The C–N stretching vibrations of the complex **2b** are found at 1450, 1428, 1413, 1373 cm^{-1} in FT-IR and 1449, 1419 cm^{-1} in FT-Raman spectrum. The theoretically calculated values of C–N stretching vibrations also fall in the region 1468–1348 cm^{-1} for **2a** and 1451–1374 cm^{-1} for the complex **2b** by B3LYP/LanL2DZ level of theory.

Conclusions

We have reported the synthesis of a bis(p-methylbenzyl)(dichloro)(1,10-phenanthroline)Sn(IV) and bis(p-chlorobenzyl)(dichloro)(1,10-phenanthroline)Sn(IV) complexes. The tin complexes having cis platin type structures are of importance in designing the anti-cancer drugs. In our complexes, the similar type of structures is confirmed as a result of the reaction. The spectral and structural studies revealed the formation of complexes in which the tin atom is hexa coordinated. Optimized geometry and vibrational wavenumbers of **2a** and **2b** complexes were studied with aid of density functional theory method with B3LYP/LanL2DZ level basis set. The various modes of vibrations are assigned unambiguously using the results of PED output obtained from the normal coordinate analysis. The calculated wavenumbers are well agreement with the experimental results. The HOMO–LUMO energy gap value suggests the possibility of intermolecular charge transfer within the complexes.

Acknowledgements

The Authors are thankful to the IISc., Bangalore and IIT Chennai, India for providing library and NMR instruments facilities usage in time. The Institute of Physics, University of Neuchatel, Switzerland is gratefully acknowledged for its service in solving structure solution of crystals.

Appendix A. Supplementary data

Crystallographic data (excluding structure factors) for the structures **2a** and **2b** have been deposited with the Cambridge Crystallographic Data Centre as supplementary publication nos. CCDC 752146 (**2a**) & CCDC 752147 (**2b**). Copies of the data can be obtained free of charge on application to CCDS, 12 Union Road,

Cambridge CB2 1EZ, UK [Fax: (internat.) +44-1223/336-033; E-mail: deposit@ccds.cam.ac.uk].

References

- [1] H.D. Yin, F.H. Li, L.W. Li, *J. Organomet. Chem.* 692 (2007) 1010.
- [2] C. Pettinari, M. Pellei, M. Miliani, A. Cingolani, A. Cassetta, L. Barba, A. Pifferi, E. Rivaola, *J. Organomet. Chem.* 553 (1998) 345.
- [3] C. Ma, J. Zhang, G. Tian, R. Zhang, *J. Organomet. Chem.* 690 (2005) 519.
- [4] J. Ouyang, Y. Xu Lian, E. Khoo, *J. Organomet. Chem.* 561 (1998) 143.
- [5] B. Krishnamoorthy, S. Chandrasekar, P. Arun Kumar, K. Panchanatheswaran, *Appl. Organomet. Chem.* 19 (2005) 186.
- [6] M.J. Frisch, G.W. Trucks, H.B. Schlegel, G.E. Scuseria, M.A. Robb, et al., Gaussian09, Revision A11.4, Gaussian Inc., Pittsburgh, PA, 2008.
- [7] M. Karabacak, M. Cinar, M. Kurt, *Spectrochim. Acta* 74A (2009) 1197–1203.
- [8] N. Sundaraganesan, S. Ilakiamani, H. Saleem, P.M. Wojciechowski, D. Michalska, *Spectrochim. Acta* 61A (2005) 2995–3001.
- [9] T. Sundius, *J. Mol. Struct.* 218 (1990) 321–326.
- [10] (a) T. Sundius, *Vib. Spectrosoc.* 29 (2002) 89–95;
(b) MOLVIB: A Program for Harmonic Force Field Calculations, QCPE Program No.807, 2002.
- [11] K. Sisido, Y. Takeda, Z. Kinugawa, in: *J. Am. Chem. Soc.* 83 (1961) 538.
- [12] IPDS-I Bedienungsbandbuch. Stoe & Cie (2000) GmbH, Darmstadt, Germany.
- [13] G.M. Sheldrick, *Acta Crystallogr. A* 64 (2008) 112.
- [14] A.L. Spek, *Acta Crystallogr. D* 65 (2009) 148.
- [15] J.C. Trehan, R.K. Sharma, C.P. Sharma, *Polyhedron* 5 (1986) 1227.
- [16] J.E. Drake, C. Gurnani, M.B. Hursthouse, M.E. Light, M. Nirwan, R. Ratnani, *Appl. Organomet. Chem.* 21 (2007) 539.
- [17] M. Khawar Rauf, M. Adeed, Imtiaz-Ud-Din, M. Bolte, A. Badshah, B. Mirza, in: *J. Organomet. Chem.* 693 (2008) 3043.
- [18] J. Holcek, A. Lycka, K. Handlir, M. Nadvornik, *Collect. Czech. Chem. Commun.* 55 (1990) 1193.
- [19] S. Calogew, L. Stievano, G. Gioia Lobbia, A. Cingolani, P. Cecchi, G. Valle, *Polyhedron* 14 (1995) 1731.
- [20] A. Tarassoli, A.F. Asadi, P.B. Hitchcock, *J. Organomet. Chem.* 645 (2002) 105.
- [21] a) M. Nadvornik, J. Holecek, K. Handlir, A. Lycka, *J. Organomet. Chem.* 275 (1984) 43;
b) T.S.B. Baul, S. Dhar, S.M. Pyke, E.R.T. Tiekink, E. Rivaola, R. Butcher, F.E. Smith, *J. Organomet. Chem.* 633 (2001) 7.
- [22] C. Pettinari, A. Lorenzotti, G. Sclavi, A. Cingolani, E. Rivaola, M. Colapietro, A. Cassetta, *J. Organomet. Chem.* 496 (1995) 69.
- [23] M.A. Buntine, V.J. Hall, E.R.T. Tiekink, *Z. Kristallogr.* 213 (1998) 669.
- [24] F.H. Allen, O. Kennard, D.G. Watson, L. Brammer, A.G. Orpen, R. Taylor, *J. Chem. Soc. Perkins. Trans. II* (1987) S1.
- [25] R.C. Poller, *The Chemistry of Organotin Compounds*, Logos Press, London, 1970, 227A.
- [26] I.R. Beattie, G.P. McQuillan, *J. Chem. Soc.* (1963) 1519.
- [27] G. Nieuwpoort, J.G. Vos, W.L. Groeneveld, *Inorg. Chim. Acta* 29 (1978) 117.
- [28] A.R. Narga, M. Schuermann, C. Silvestru, *J. Organomet. Chem.* 623 (2001) 161.
- [29] J.E. Huheey, *Inorganic Chemistry Principles of Structure and Reactivity*, second ed., Chap. 6, Harper & Row, New York, 1978.
- [30] S.G. Teoh, S.B. Teo, G.Y. Yeap, J.P. Declercq, *Polyhedron* 11 (1992) 2351.
- [31] H. Fujiwara, F. Sakai, Y. Sasaki, *J. Chem. Soc. Perkin Trans. II* (1983) 11.
- [32] K. Ueyama, G.-E. Matsubayashi, R. Shimizu, T. Tanaka, *Polyhedron* 4 (1985) 1783.
- [33] U. Casellato, R. Graziani, M. Martelli, G. Plazzogna, *Acta Crystallogr. C* 51 (1995) 2293.
- [34] L.E. Smart, M. Webster, *J. Chem. Soc., Dalton Trans.* (1976) 1924.
- [35] P. Thul, V.P. Gupta, V.J. Ram, P. Tandon, *Spectrochim. Acta* 75 (2010) 251–260.
- [36] P. Politzer, J.S. Murray, in: D.L. Beveridge, R. Lavery (Eds.), *Theoretical biochemistry and molecular biophysics: a comprehensive survey*, protein, 2, Adenine Press, Schenectady, New York, 1991.
- [37] P. Politzer, J. Murray, *Theor. Chem. Acc.* 108 (2002) 134–142.
- [38] A.D. Becke, *J. Chem. Phys.* 98 (1993) 5648–5682.
- [39] C. Lee, W. Yang, R.G. Parr, *Phys. Rev. B* 37 (1998) 785–789.
- [40] Y. Ataly, D. Avci, A. BaSoglu, *J. Struct. Chem.* 19 (2008) 239–246.
- [41] T. Vijayakumar, I. Hubert Joe, C.P.R. Nair, V.S. Jayakumar, *J. Chem. Phys.* 343 (2008) 83–99.
- [42] G. Varsanyi, *Assignments for vibrational spectra of seven hundred benzene derivatives*, 1, Adam Hilger, London, 1974.
- [43] P.S. Kalsi, *Spectroscopy of Organic Compounds*, Wiley Eastern Ltd., New Delhi, 1993.
- [44] N.B. Dudley, H. Williams, Ian Fleming, *Spectroscopic Methods in Organic Chemistry*, Tata McGraw-Hill, UK, 1988.
- [45] I. Matulkova, I. Nemec, K. Teubner, P. Nemec, Z. Micker, *J. Mol. Struct.* 873 (2008) 46–60.
- [46] R.C. Mehrotra, A. Singh, *Organometallic Chemistry*, New Age International (P) Ltd Publishers, New Delhi, 2004.